NEW PANDA INSTRUMENTATION FOR ASSESSING GAS CONCENTRATION DISTRIBUTIONS IN CONTAINMENT COMPARTMENTS

M. Ritterath [a1], H.-M. Prasser[a], D. Paladino[b], N. Mitric[a]

a) ETH Zürich, Sonneggstr. 3, 8092 Zürich, Switzerland
b) Paul Scherrer Institut, 5232 Villigen, Switzerland

Abstract: The increased use of CFD for analysis and design purposes demands high quality data to validate the code's results. The present paper introduces a measuring system able to characterize the gas composition and to withstand the rough conditions inside a large-scale containment test facility. The speed of sound in ideal gases is a function of the gas composition. Out of the measured time of flight of an ultra sound pulse between a pair of transducers the integral speed of sound along the chord spanned between the transducers is computed. This quantity characterizes the gas composition and therefore can be used for model validation purposes even though concentrations of individual components cannot be resolved in cases of more than a binary mixture. The results of preliminary tests specifying the measurement system's properties are discussed.

1 INTRODUCTION

The actual trends in reactor safety research show a wide use of CFD codes. Growing calculation power allows the application of CFD also for containment analyses. Experimental data needed for code validation have to be obtained preferably from large scale tests, minimizing the impact of scaling distortions in the assessment of the CFD models. Phenomena such as fluid (air, steam, hydrogen) stratification in the containment as well as break-up of stratification induced by negatively buoyant flow, gas transport between containment compartments, wall condensation, etc. have been identified as high-ranking phenomena playing an important role in issues directly related to the safety or to the design of future reactors (Yadigaroglu et al., 2003). In the frame of the OECD/SETH-2 project the large scale test facility PANDA, located at Paul Scherrer Institute in Switzerland, is used for an experimental program investigating phenomena relevant for LWR containment safety (Paladino et al., 2008). The PANDA instrumentation allows to measure fluid temperature, velocity, gas concentration, etc. in challenging situations arising from the fluid conditions inside the facility (pressures up to 1 MPa and temperatures up to 200°C) and in presence of multi-component mixtures (air, steam, helium). Specific test scenarios characterized by steam condensation challenge further the use of measurement techniques such as the PIV system for fluid velocity or Mass Spectrometer (MS) for gas concentration measurements. The mass spectrometer is connected to a pre-selected set of 38 capillaries taking samples from various positions inside PANDA. The capillaries are multiplexed to the analyzer successively. Due to the slow convergence of the MS measurement the resulting sampling period is up to 380 s when all capillaries are sampled.
In a research cooperation between ETH Zürich and PSI new sensors are under development that are suitable for the characterization of the gas composition in large volume vessels such as those of PANDA facility. With respect to the gas measurements currently performed using the MS, the new sensors will allow a higher frequency for the data acquisition. Figure 1 shows the vessels of PANDA which will be used in the SETH-2 tests. The upper two vessels in Figure 1 are connected by a pipe of large diameter (80 cm). In total these two vessels and the interconnecting pipe have 180 m^3 total volume.

The final goal of the current R&D for the new sensors is to obtain quantitative information characterizing the multi-component gas compositions in large volumes (like PANDA compartments) with a sufficient high frequency. The high frequency is necessary to capture the timing for the gas stratification break-up or for fast transient scenarios. The timing of gas stratification break-up is one of the parameters which can be directly compared with 3D code predictions. The new sensors are suitable e.g. for tests aiming at studying the behavior of a stratified layer of hydrogen, accumulated as a consequence of a core damage accident. Such test series are under preparation in PANDA facility (Paladino et al., 2008). In these tests the formation of an helium-rich layer (helium being the model fluid for hydrogen) in the upper volume of a PANDA compartment will be postulated and the possibility to break the helium stratification by the vertical release of steam that become negatively buoyant after impinging on the helium layer will be investigated.

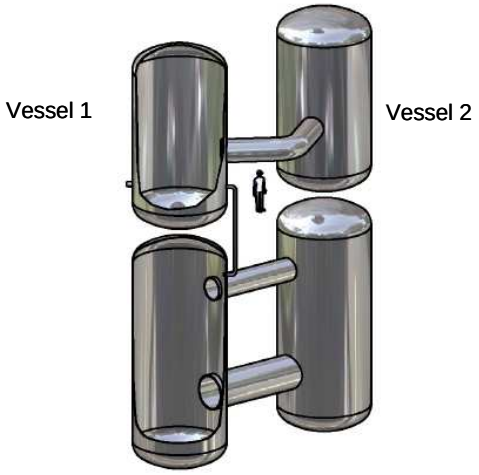

Figure 1: PANDA facility. The upper left vessel is the one where the measurement system will be installed.

2 SPEED OF SOUND MEASUREMENT

The speed of sound of an ideal gas is depending on its molecular mass M, the adiabatic exponent k and its temperature T like shown in equation 1

$$c_{gas} = \sqrt{\frac{k \cdot R \cdot T}{M}} \,. \tag{1}$$

In mixtures of gases the adiabatic exponent k and the molecular mass M are functions of the fractions x_i of its components

$$k = \sum_{\mathrm{i}} \frac{x_{\mathrm{i}} \cdot k_{\mathrm{i}}}{k_{\mathrm{i}} - 1} \Bigg/ \frac{x_{\mathrm{i}}}{k_{\mathrm{i}} - 1} \tag{2}$$

$$M = \sum_{\mathrm{i}} x_{\mathrm{i}} \cdot M_{\mathrm{i}} \,. \tag{3}$$

From equations 1 – 3 follows that at a given temperature the speed of sound is a unique function of the concentration ratio and in case of a binary gas mixture this function is one to one. Often, the containment atmosphere is a mixture of more than two components. In such cases, the gas concentration vector cannot be resolved into its single components by only one independent parameter like the speed of sound, but the speed of sound can serve as a quantity characterizing

the gas composition. Measured speed of sound data can be used for code validation purposes, which is often the main goal of the experiments. To do so, the results of the model calculations, delivering theoretical values of the concentrations of all participating gases can be transformed into a speed of sound. The distribution and transient change can be compared to the measuring results in order to draw conclusions on the model accuracy and reliability.

3 TRANSDUCERS FOR SPEED OF SOUND MEASUREMENT

The transducers (see Figure 2) for the speed of sound measurement were developed by Melnikov et al. (2006). They work in a similar way like speaker and microphone. They are based on lead-zirconat-titanat piezoelectric crystals accommodated in a tight cylindrical stainless steel case. On one end there is a conical wave-guide conducting the sound towards a transversal resonance plate serving as an "antenna" for the ultrasound. On the opposite end there is a cylindrical resonance body helping to direct most of the energy towards the antenna. The transducers are tuned to a frequency of 37 kHz. This near ultrasound is able to be irradiated into a gaseous medium. Transmitters and receivers are identical. To avoid body sound transmission, a piece of silicon resin foam has to be put between the foot of the transducer and the fixing gadget.

Figure 2: Ultrasound transducer with silicon foam and fixing gadget.

3.1 Measuring Principle of the System

The speed of sound is measured between pairs of transducers mounted in a certain distance from each other. Following a given pattern, each transducer will emit a pulse of sound while the remaining transducers are receiving. Figure 3 shows a schematic of the system.

To emit a sound pulse, the CPU selects via the de-multiplexer (Demux) one of the 32 channels. The 37 kHz sinusoidal signal from the sinus generator is forwarded to the selected channel and transformed to an amplitude of 600 V_{pp}. Because of this signal the piezoelectric crystal inside of the transducer oscillates and the vibration propagates through the wave guide to the sound plate.

Due to the oscillations orthogonal to the plate bending waves are excited and propagate towards the ends of the sound plate. These bending waves irradiate sound into the surrounding gas under the angle (Melnikov, 2006)

$$\cos\alpha = \frac{c_{gas}}{c_{bend}} \tag{4}$$

from the plate, where the propagation speed of the bending waves is defined by (Cremer, 1967)

$$c_{bend} \approx \sqrt{1.8 \cdot c_{metal} \cdot h \cdot f}\ . \tag{5}$$

c_{metal} denotes the longitudinal sound speed inside of the sound plate in axial direction, h denotes the thickness of the sound plate and f the excitation frequency. The bending waves are reflected at the end of the sound plate creating a pattern of superposed waves. The duration of the sound pulse is adjustable, typically in the range of 1 ms.

For the receivers the principle of the transducers is reversed, i.e. the sound plate of the receiving transducer is excited to bending oscillations forwarded through the wave guide to the piezoelectric crystal. Being deformed the crystal emits electrical charges. The charges are amplified and pulse shaped in a way that the output signal represents the envelope of the received sinusoidal sound signal. The output signals as well as the digital edge of the send pulse are recorded with a sampling frequency of 78 kHz, which represents the maximum sampling frequency available with the data acquisition.

With this procedure of exciting all transducers after each other while the others are receiving a distribution of the integral sound speed measured along the chords spanned between the transmitter and the receivers is obtained.

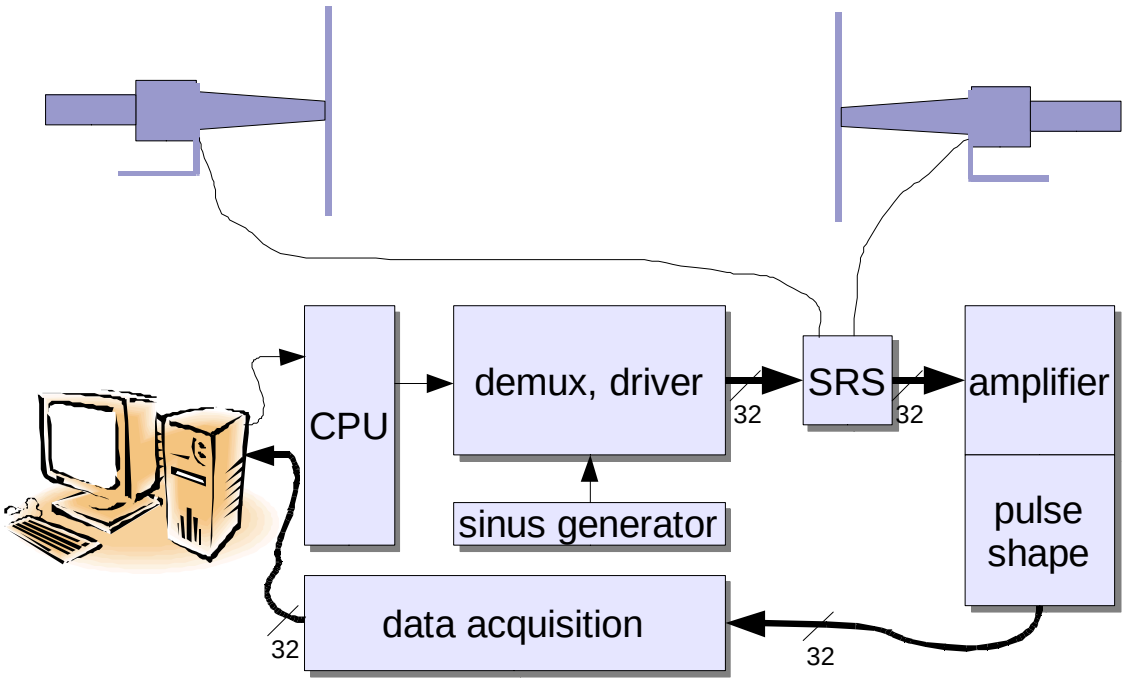

Figure 3: Block diagram of the measuring system consisting of the transducers, the transmitter and the receiver part. These last two parts are separated by the send receive separator (SRS).

It is in the nature of the time of flight measurement to sample an integral measure along the chord spanned between emitter and receiver. The loss of the one dimensional distribution information along the chord is compensated for by the better time resolution of 1 Hz compared to the installed

mass spectrometers (380 s per frame). The sampling rate is limited to about 1-2 Hz for the entire ultrasound system due to the reverberation time of the transducers and the vessel volume.

3.2 Data Evaluation

The aim of the measurement is to deliver a speed of sound distribution. The speed of sound is computed out of the time of flight that is derived from the recorded signals like shown in Figure 4. The green plotted signal output from the pulse shaping part of the receive unit is gained inside the receiver by an analog filter by cutting off the negative half wave of the incoming charges and low passing the positive component of the signal. The output signal shows two components. One is the superposition of direct sound and echo and forms the envelope. The high frequency with the small amplitude superposed is the received excitation frequency damped after the low pass filtering.

The time of flight *TOF* is assumed to be the time difference between the positive edge of the send pulse and the moment when the received signal starts to rise (see Figure 4). It is well known that a bend in a signal has a local extremum in the 2nd derivative of the signal as well as it is known that deriving a noisy signal is challenging. In the present case the second derivative is gained using the acausal Savitzky-Golay-filter algorithm (Sterliniski, 1974) with a width of 101 and an order of 7. This filter consists of a core that is symmetrically convoluted with the signal. The 2nd derivative is plotted in red below the signals (Figure 4). The avoid uncertainties from the noisy signal a smoothing function is fit into the 2nd derivative. The first local minimum of this smoothed function after the signal fell below a noise cutting threshold denotes the moment when the pulse arrives at the receiving transducer. The time of flight *TOF* now can be computed as

$$TOF = \frac{n_{sample}}{f_{sampling}} \tag{6}$$

with n_{sample} denoting the position of the local minimum and $f_{sampling}$ denoting the sampling frequency of the data acquisition. From equation 6 the speed of sound

$$c_{measured} = \frac{s}{TOF} \tag{7}$$

can be calculated, where s denotes the distance between the transducer pair.

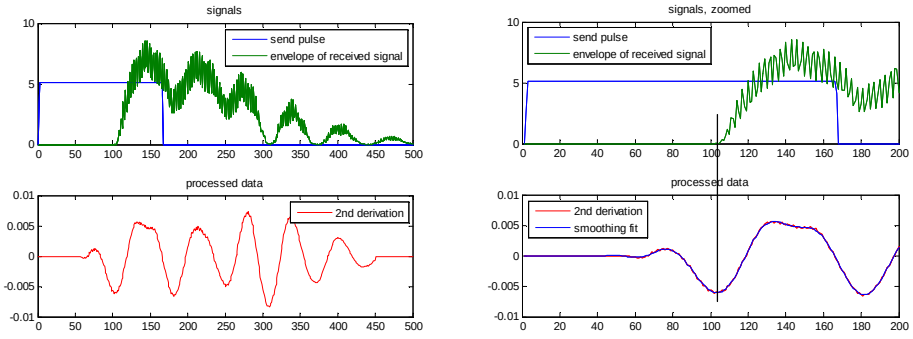

Figure 4: a) Recorded raw data. Blue: duration of send pulse, Green: output signal of the receiver unit, Red: 2nd derivative of Green. b) Zoom of signals. All signals are plotted versus time (timescale 80 kS/s).

3.3 Sensor tests

Up to now three different kinds of sensor tests have been carried out:

- tests to prove the ability of the transducers to withstand the conditions inside Panda,
- calibration tests in air with different set-ups and
- calibration tests in helium with a constant set-up.

In order to prove the transducers can withstand the conditions inside PANDA compartments two transducers have been mounted inside PANDA during several preliminary tests under conditions prototypical of the tests foreseen in the frame of the OECD/SETH-2 project. The sensors' behavior was observed and showed no conspicuities. It has been noted that for test conditions characterized by extensive steam condensation, it may occur that water drops deposit on the sound plates and distort the resonance frequency so that no signal is received anymore. As soon as the water drops evaporate the transducers came back to function again.

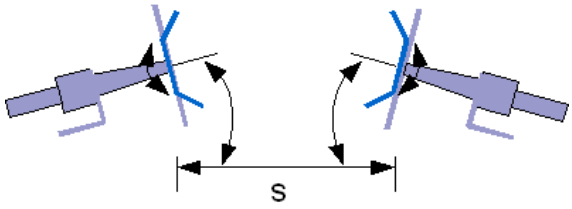

Figure 5: Sketch of varied parameters for measuring the directional characteristic.

In a second test the sensors have been installed in different distances from each other to check the accordance of the theoretical time of flight TOF_{theor} as function of distance against the measured time of flight $TOF_{measured}$. Also the orientation and the shape of the sound plate, the angle of the emitter to the receiver and the angle between emitter and receiver have been varied for determining the directional characteristic. The evaluation of the data, done as described before, delivered a set of measured times of flight $TOF_{measured}$. These values have been compared with theoretical values TOF_{theor} computed from equation 8

$$TOF_{theor} = \frac{s}{c_{air}} \tag{8}$$

where s again denotes the distance between the transducers (see Figure 5) and c_{air}, the sound speed in air was assumed to be 343 m/s (see Figure 6). The delay

$$D = TOF_{measured} - TOF_{theor} \tag{9}$$

is plotted versus the distance between the transducers in Figure 9.
The delay is independent from the orientation of the sound plates but shows a dependency from the distance, which is stronger for the straight sound plates than for the bended sound plates. Between the transducer's positioning angles and the delay no correlation has been found. At the present state of the investigations it is postulated that the delay is the consequence of the build-time of the oscillators and the sound plates. This postulation is consistent with the observation that the delay is a function of the distance since the power density is decreasing with the distance. For the bended sound plates the power density decrease is less accentuated so the delay does not increase that much like using straight sound plates.
The transducers have been tested in all relative positions to each other that are foreseen for the experiments in PANDA and in all the varied set-ups performed properly.

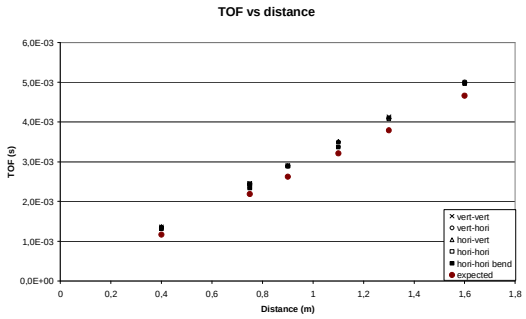

Figure 6: time of flight plotted against the distance and compared with the expected values.

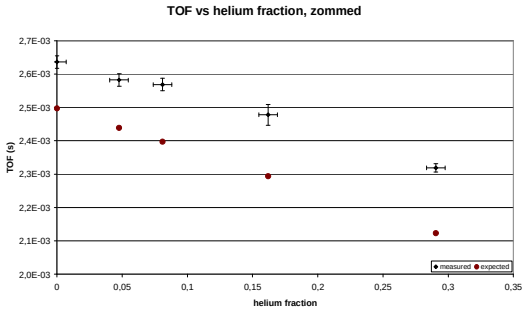

Figure 7: time of flight plotted against the helium fraction and compared with the expected values.

With the third preliminary test the accordance of the theoretical time of flight TOF_{theor} as a function of helium concentration with the measured time of flight $TOF_{measured}$ was investigated. The experiment was carried out in the commissioning chamber "Pandalino" at ETH (see Figure 8). This chamber has an octagonal ground plane with a diameter of 2.96 m, a height of 2.35 m and a volume of 14.6 m^3. It is equipped with a helium supply, a ventilator and an oxygen probe. Pandalino is designed for zero overpressure and temperatures up to 80°C. The ventilator guarantees an equal distribution of the helium inside Pandalino so that the measurement of the oxygen sensor is representative for the whole volume. Out of the oxygen fraction fr_{oxygen} one can calculate the helium fraction fr_{helium} under the assumption that only helium replaces the air

$$fr_{helium} = 1 - \frac{fr_{oxygen}}{0.21}. \tag{10}$$

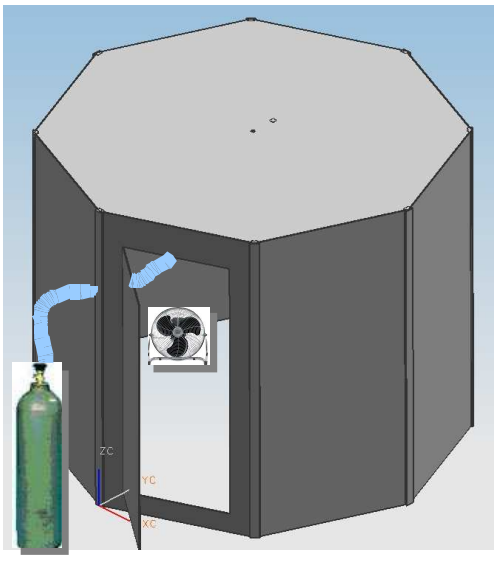

Figure 8: Pandalino with helium supply and fan.

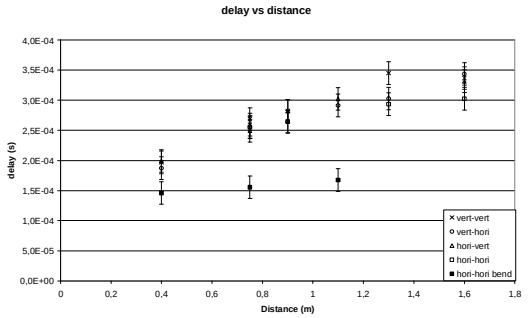

Figure 9: Delay of signal receipt vs. the distance. "Vert" denotes that the sound plate was vertically oriented - "hori" denotes that the sound plate was horizontally orientated. The transmitter is mentioned first. The error bars quantify the scatter during a set of 100 measured times of flight.

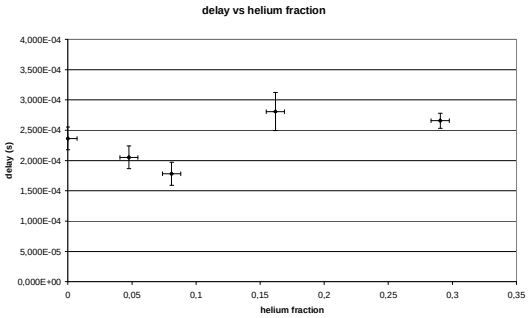

Figure 10: Delay vs. helium fraction. The error bars for the delay quantify the scatter during a set of 100 events within a helium fraction. The error bars for the helium fraction denote the uncertainty of the helium fraction.

For the experiment that has been carried out at a temperature of 23°C Pandalino was filled stepwise with helium while the transducers mounted with bended sound plates have been placed inside at a distance of 0.86 m. The measured time of flight $TOF_{measured}$ was compared with the theoretical time of flight TOF_{theor} which was computed with the help of equation 1-3 and 10. The comparison shows a high accordance (see Figure 7) between the theoretical and measured time of flight with respect to the delay. The already described delay is plotted in Figure 10 versus the helium fraction.

In Figure 9 we see a variation of the build time in the range from 0.15 ms to 0.35 ms due to set-up changes under constant conditions and in Figure 10 due to condition changes at a given set-up, respectively. The variations are within each measuring point very small.

The variations of the delay shown in Figure 10 occurring at a constant set-up are caused by the fact that the heterogeneous energy distribution field of the transmitter is opened up due to the sound speed dependant irradiating angle of sound caused by bending waves (equation 5). This opening causes the receiver to be placed in areas with different energy densities expressed by a variation in the delay.

4 DISCUSSION OF UNCERTAINTIES

The total differential of equation 7 divided by equation 7 itself

$$\frac{\Delta c_{measured}}{c_{measured}} = \left|\frac{\Delta s}{s}\right| + \left|\frac{\Delta TOF_{measured}}{TOF_{measured}}\right| \tag{11}$$

shows us the contributions to the uncertainty of the measured speed of sound where Δs denotes the uncertainty of the distance between transmitter and receiver caused for example by uncertainties in the positioning or shifts due to thermal expansion of the vessel and fixing gadgets. $\Delta TOF_{measured}$ denotes the uncertainty of the time of flight measurement. It consists of the scatter during one set-up at constant conditions and of the scattering caused by the displacement of the energy distribution field as uncertainty while in contrary the set-up dependant scattering illustrated in Figure 9 is to be compensated for by a calibration under given conditions.

Table 1 summarizes the values of the absolute uncertainties evaluated at a distance of 0.86 m.
The resolution of the time of flight measurement is limited by the sampling frequency of the data acquisition system that is 78 kHz.
Consider a binary mixture of air and helium where the helium fraction doesn't exceed 40% and the pair of transducers is at least at a distance of 1.2 m from each other (PANDA conditions). Then the sampling time of approximately 13 µs results in a resolution of helium fraction steps between 1.5% and 2%. In this described case the uncertainty in the speed of sound leads to an uncertainty of about 6% helium fraction. To compensate for the low accuracy the data can be adjusted by data from the mass spectrometer installed at Panda, too.

Table 1: uncertainties

Δs	12 mm
$\Delta TOF_{measured}$ (scatter within a set-up under constant conditions)	31 µs
$\Delta TOF_{measured}$ (scatter due to distribution shift)	50 µs
Total relative uncertainty $\Delta c / c$	$< \pm$ 6%

5 PLANNED TESTS IN PANDA FACILITY

5.1 Experiment Description and Sensor Positions

Before the experiment starts the facility is pre-conditioned to have a steam and helium rich layer in the upper part of vessel 1 (DW1, upper left vessel in Figure 1). The remaining volume of vessel 1, the interconnecting pipe and vessel 2 are filled with steam only.
During the experiment superheated steam or air will be released into the upper vessel volume through a vertical injection line that has its exit in the upper part of the vessel. The injected fluid (steam) will due to its negative buoyancy penetrate after a certain time the helium rich layer and expand this layer downwards by weakening it, too, depending from the injections parameters. The tests will be performed at constant pressure, i.e. during the injection in vessel 1 a fluid mixture (helium-steam) is vented out from the upper part of vessel 2 (see Figure 1).
The 30 transducers will be placed in three different groups called "columns", "rings" and "IP" like shown in Figure 11.
Fourteen of the transducers are scheduled to be placed in two vertical columns with each seven transducers arranged in pairs at the same levels. The levels are below the helium steam rich layer. The plane spanned by the columns will be located at the side remote from the interconnecting pipe to avoid disturbances from the interconnecting pipe entrance.
Another twelve transducers will be mounted on two concentric rings above the opening of the steam/air injection pipe. On each ring six transducers are equally distributed.
The remaining four transducers will be placed shortly behind the entrance of the interconnecting pipe.

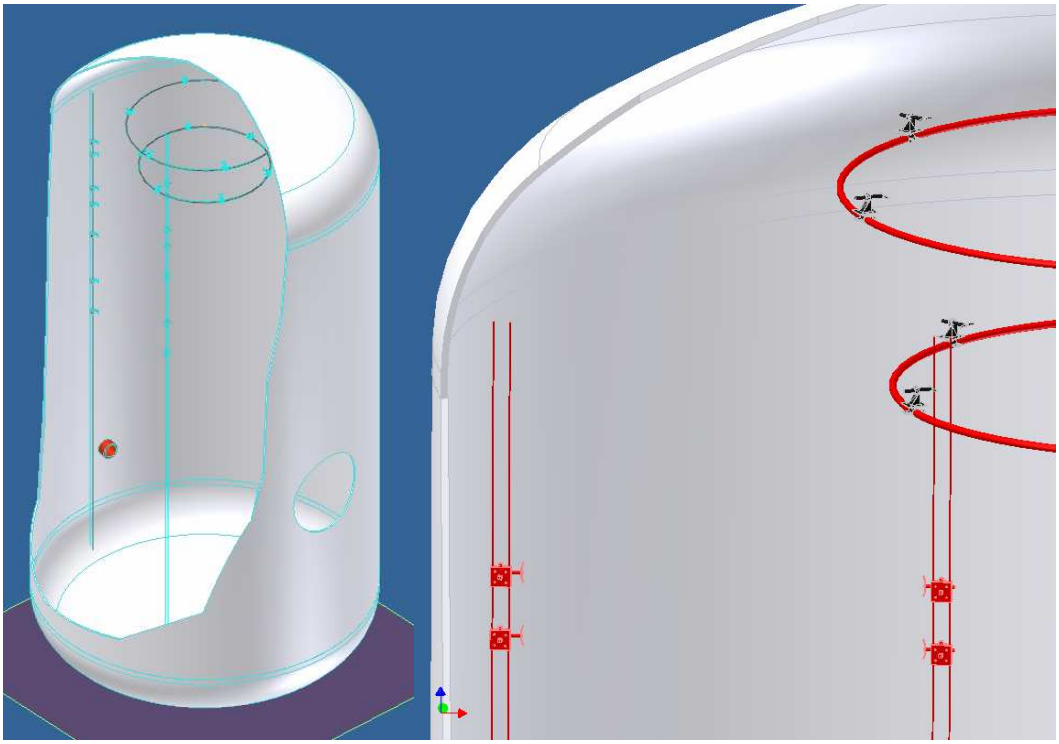

Figure 11: Sensor positions inside PANDA.

5.2 Objectives Addressed with the Arrangement Described above

With the transducers on the columns it is possible to capture the horizontal oscillations of the formation of the helium stratification with higher frequencies. Furthermore the speed of the downwards movement of the stratification layer can be evaluated.
With the transducers mounted on the rings it is possible to detect the moment when the vertical low momentum jet penetrates the helium rich layer in the upper part of the vessel. Additionally the bending angle of the jet can be detected.
The four transducers at the entrance of the interconnecting pipe give a measure about which gas composition is leaving vessel 1 and if there is a stratification in the flow through the IP.
Though the measuring resolution and the accuracy of the introduced measurement system are limited it will contribute considerably to the validation of the CFD models due to the better time resolution and the ability to capture the moments of flow pattern changes.

6 SUMMARY

The paper presented the status of development for the implementation of new sensors for gas concentration measurements in large volume vessels like those of PANDA facility. The sensor principle is based on the dependence of speed of sound from the gas compositions. The tests performed so far identified the sensor response as a function of different parameters named the fluid conditions and geometrical parameters. From instance it has been found out that in presence of a fluid atmosphere characterized by a large amount of steam condensation, the deposition of water drops on the sensor can inhibit temporarily its functioning. The variation of geometrical parameters such as the relative angle between the sensors seems to have a minor effect on the delay with respect to the variation of sensor distance.

Other qualification tests are undergoing in the Pandalino facility aiming to quantify the accuracy of the sensors in measuring the gas concentrations. The main advantage by using these sensors with respect to the mass spectrometer is the higher frequency of the data acquisition. For specific experiments characterized by fast transients the timing for breaking up an initially helium rich stratified layer is one of the main parameters that can be used for a 3D code validation. In this prospective, the new sensor for gas concentration measurements would contribute to the generation of an experimental database for validating codes with 3D capability against phenomena relevant to LWR containment safety.

REFERENCES

O. Auban, D. Paladino, "Description of PANDA gas concentration measurement system using mass spectrometry" *PSI Report* TM-42-01-11 ALPHA-01-01, 2002

L. Cremer, "Körperschall – Physikalische Grundlagen und Technische Anwendungen" Springer-Verlag, Berlin, 1967

S. Sterlinski, "General formulas for calculation of Savitzky and Golay's filter weights and some features of these filters", Nuclear Instruments and Methods 124, 1974

V.I. Melnikov, V.P. Drobkov, V.V. Kontelev, "Akusticeskie Metodi Diagnostiki Gazozidkoctnjih Potokov" *Energoatomizdat* (2006), Moskva, ISBN 5-283-00807-X

D. Paladino, M. Huggenberger, M. Andreani, S. Gupta, S. Guentay, J. Dreier, H. Prasser, "LWR Containment safety research in PANDA", submitted for the proceeding of International Congress on Advances in Power Plants (ICAPP 08)-Anaheim, CA USA, June -12, 2008

G. Yadigaroglu, M. Andreani, J. Dreier, P. Coddington, "Trends and needs in experimentation and numerical simulation for LWR safety*", Nuclear Engineering and Design*, **Vol. 221,** pp. 205-223 (2003).

[1] Corresponding author: Martin Ritterath, Ritterath@lke.mavt.ethz.ch, Tel: 0041 44 63 24901